Power electronic traction transformers in 25 kV / 50 Hz systems: Optimisation of DC/DC Isolated Converters with 3.3 kV SiC MOSFETs

Florent Morel, Caroline Stackler, Philippe Ladoux, Alexis Fouineau, François Wallart, Nathan Evans, Piotr Dworakowski

Power electronic traction transformers in 25 kV / 50 Hz systems: Optimisation of DC/DC Isolated Converters with 3.3 kV SiC MOSFETs

Florent MOREL[1,2], Caroline STACKLER[2,3], Philippe LADOUX[3], Alexis FOUINEAU[1,2], François WALLART[2], Nathan EVANS[2], Piotr DWORAKOWSKI[2]

[1] Univ Lyon, École Centrale de Lyon, Université Claude Bernard Lyon 1, CNRS, Ampère, France
[2] ITE Supergrid Institute SAS, France
[3] Université de Toulouse, Laplace, France

Corresponding author: Florent MOREL, florent.morel@supergrid-institute.com

The Power Point Presentation will be made available after the conference.

Abstract

In AC electric trains, power electronic traction transformers (PETT) are multilevel single phase AC/DC converters connected to the AC medium voltage overhead line. For indirect topologies, DC/DC isolated converters are key elements of PETTs. This paper shows a method to design such DC/DC converters, and several variants are considered. Finally, the comparison results, in the case of a 25 kV / 50 Hz power supply and 3.3 kV SiC MOSFETs, show that the variant with a resonant AC link, with only one controlled bridge and a switching frequency lower than the resonant frequency, offers the best efficiency at rated power for a given volume.

1 Introduction

On AC railway infrastructures, an on-board power converter is required between the overhead line and a DC traction bus, on which are connected three-phase inverters supplying the traction motors. Currently, this is done by a step-down transformer directly connected to the overhead line, and full bridge AC/DC converters based on silicon IGBTs and diodes [1]. Recently, many research works have been carried out [2]–[5] in order to find alternatives to this well-known solution, to improve the efficiency of the transformer, limited by the on-board volume constraint (especially in the case of 15 kV / 16.7 Hz power supply) [1].

Among the different topologies found in the literature [2]–[5], the power electronic traction transformer (PETT) considered in this work is depicted in Fig. 1. This is a modular converter built with power electronics building blocks (PEBB). Each PEBB includes an AC/DC stage (active front end converter (AFEC)) and an isolated DC/DC converter. These blocks are connected in series on the AC side to withstand the overhead line voltage, and in parallel on the DC side to supply the traction bus. In this solution, the transformers are supplied by medium frequency voltages and are then named *medium frequency transformers* (MFT). The expected advantages of this solution are a reduction of the volume and mass constraints on the transformer, and thus, a higher efficiency of the converter under given volume and mass constraints.

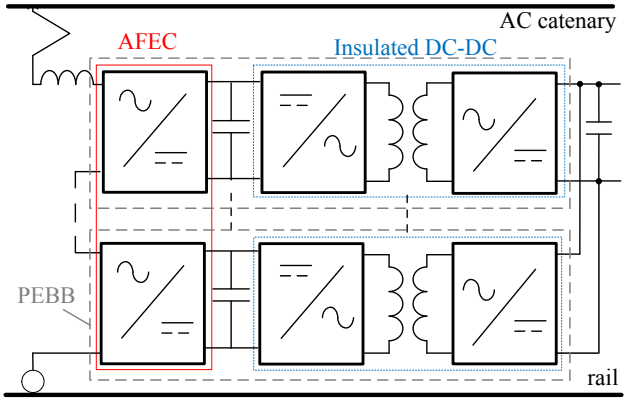

Fig. 1: Considered topology of PETT

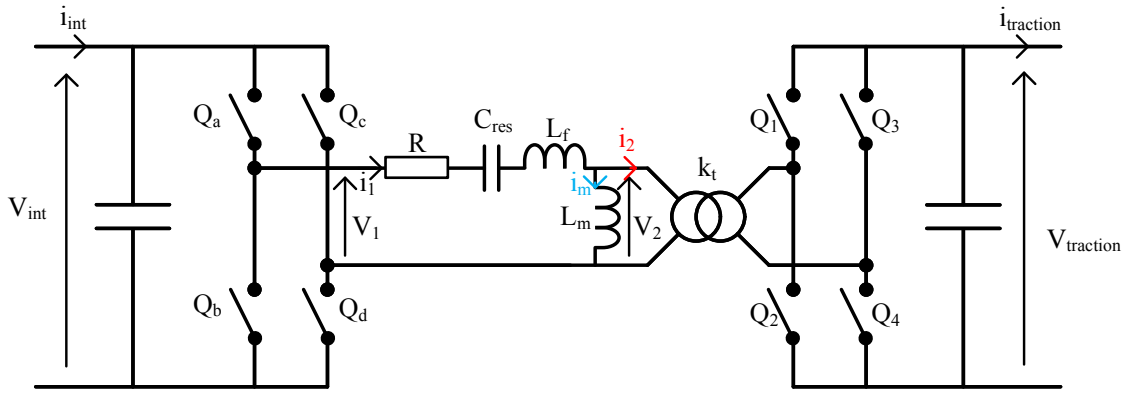

Fig. 2: DC/DC stage circuit (Note that for the NR-DAB case, the capacitor C_{res} is omitted.)

This paper is focused on the DC/DC stages of a PETT. To our best knowledge, in the literature on PETTs, there is no paper giving much detail on this part of the converter. As it will be shown in section 2, some variants are possible. The goal of this work is then to optimize the design of these converters (MFT core material, core size, windings, switching frequency...) in order to obtain the best efficiency in a given volume and eventually to identify the variant which leads to the best efficiency. The original contributions of this work include the assessment of silicon carbide (SiC) MOSFETs for this kind of converters. The methodology used and the models are presented in section 3. Results are given and discussed in section 4. Finally section 5 highlights the conclusions of this study.

2 Considered variants

The general representation of the considered DC/DC converters is given in Fig. 2, where switches are 3.3 kV SiC MOSFETs. This is a *resonant dual active bridge (R-DAB)*. In a first variant, the resonant capacitor can be omitted; this variant will be named *non resonant dual active bridge* (NR-DAB). In these variants, the RMS values of V_1 and V_2 are supposed equal and the phase shift between both bridges should be controlled with a high precision, requiring a high performance computing unit.

To reduce this constraint, the other variants consist in controlling only one bridge among both full bridges (switches Q_a to Q_d in traction mode, switches Q_1 to Q_4 in braking mode), the second one operating as a diode bridge (using MOSFET body diodes or additional SiC Schottky diodes according to the module supplier). These cases, often named *full-bridge LLC resonant converter* in the literature, are named *resonant single active bridge* (R-SAB) in this paper. In these cases, $V_{traction}$ is supposed constant while V_{int} slightly varies according to the transmitted power. The switching frequency can be chosen lower or higher than the resonant frequency of the AC link. These operating modes are named *discontinuous current mode* (DCM) and *continuous current mode* (CCM) respectively.

The case of non resonant single active bridge is not considered in this work because it has been shown in [6] that the high impedance of the AC link (between V_1 and V_2) leads to too large voltage drops.

In any considered cases, when a bridge is controlled, it generates a voltage with a rectangular shape (e.g. V_1 equals $\pm$ V_{int} but is never null). All the considered cases leads to different current shapes, as shown in Fig. 3, leading to different constraints on semiconductors and transformers.

In order to identify the best variant, an optimisation process should be run for each considered case. This has been done using the methodology presented in next section.

3 Methodology and hypotheses

The methodology used to compare the considered variants is the same as the one presented in [7] but more details are given in here. The goal is to obtain the best efficiency at rated power within a given volume and a given mass. For this, an optimisation process is run for different switching frequencies. The flowchart is presented in Fig. 4.

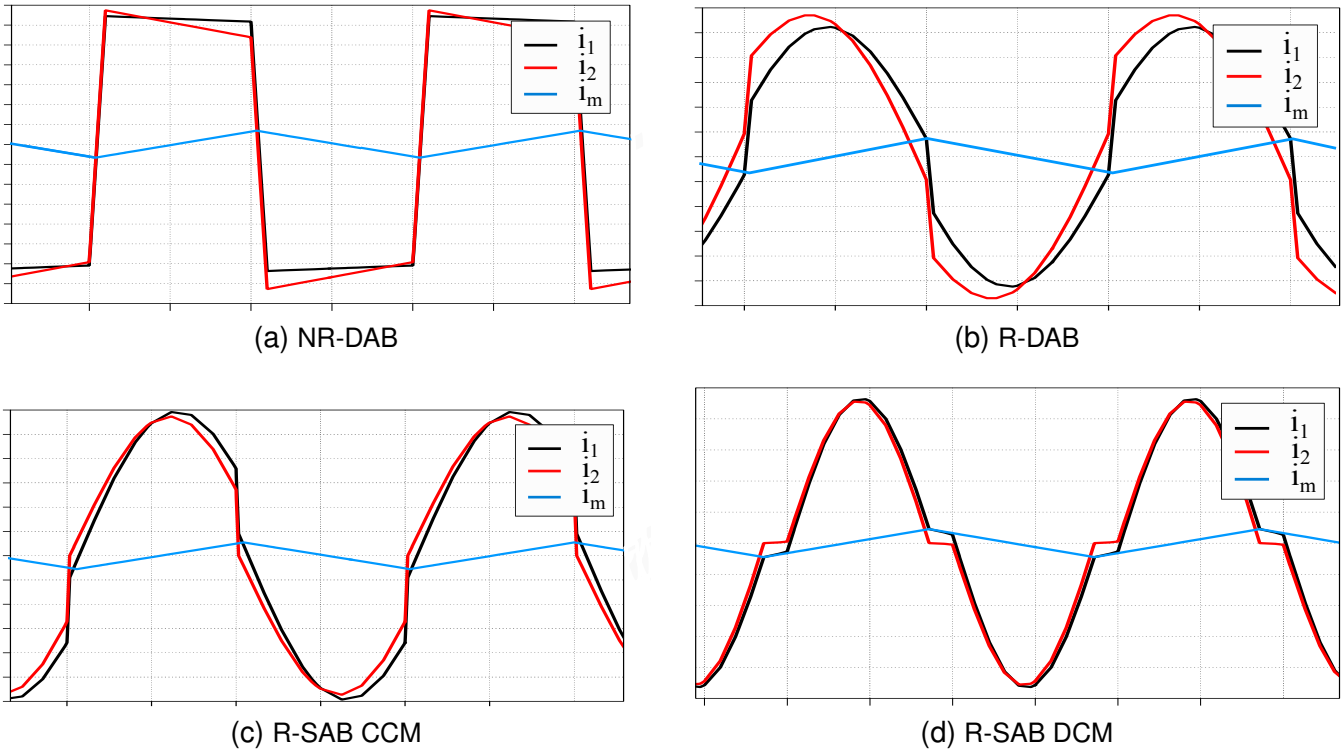

(a) NR-DAB (b) R-DAB

(c) R-SAB CCM (d) R-SAB DCM

Fig. 3: Current shapes for the considered cases in traction mode (Note that here the magnetizing inductance has been chosen lower than for a real application to highlight the impact of the magnetizing current.)

The procedure starts with calculating the constraints on the magnetizing and leakage inductances.

The magnetizing current is related to losses and zero voltage switching (ZVS), especially for the case of R-SAB DCM where the magnetizing current is the switched current. A particular attention was given to the calculation of this current for all the considered variants. In the following, only transformers that present a magnetizing inductance low enough to allow a ZVS operation whatever the transmitted power are considered (The magnetizing current should be large enough to charge and discharge C_{DS} capacitances during dead times.).

The leakage inductance is also constrained. In DAB mode, it is a trade-off between the smallest realisable time-shift between both bridge voltages (limited by the performances of the control computing unit), and the maximal phase-shift between these voltages (limited because, for the control, the model is supposed linear). In SAB mode, the higher the AC link (R, C_{res}, L_f) impedance, the higher the voltage drop on the intermediate buses.

According to these values, current and voltage shapes are calculated thanks to analytic expressions. For this, the magnetizing inductance is supposed equal to the maximal value calculated above; in DAB mode, the considered leakage inductance is the minimal value (that leads to the rated power with the minimal allowed time-delay); in SAB mode, the considered leakage inductance is the maximal value (that leads to the maximal voltage drop on the DC intermediate bus). In the cases of R-DAB and R-SAB in traction mode, no analytic solution was found for the initial conditions of the differential equations. Thus, in these cases, these constants are calculated thanks to an iterative method (consider some values for initial conditions, solve the differential equations, get the final values and solve again equations with these values as new initial conditions and so on until convergence) validated in simulation.

Then several pre-designs of medium frequency transformers (MFT) are generated. To do so, an analytical design process is followed. The degrees of freedom for this design are magnetic induction, current densities, number of turns and

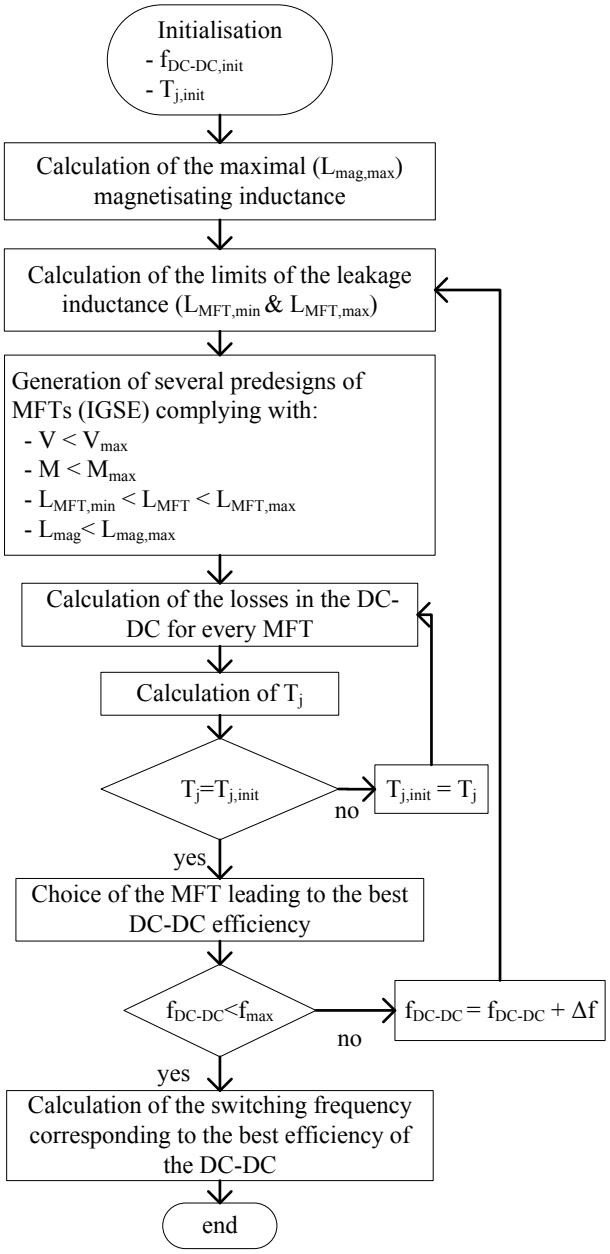

Fig. 4: Flowchart of the sizing of each DC-DC converter

form factors. Therefore, the degrees of freedom are swept over a wide range, ensuring they remain in realistic values, to obtain an important number of potential MFT designs, around 100,000 to 1 million. For each potential design, inductances, parasitic capacitances, losses and temperatures must be calculated to determine if the transformer will respect the performance criteria previously established.

The magnetizing and leakage inductances are calculated from the classical reluctance evaluation method, considering that the direction of the magnetic field is normal to the magnetic core cross-section, an assumption which is typically valid for core-type geometries. The parasitic capacitances (which have to be evaluated for dielectric losses calculation) are calculated in the same way, by assuming that the electric field is normal to the surface of conductors. A plane-plane capacitor formula, including edge effects, is considered between primary and secondary windings, and also between each turns of laminated Litz cables.

There are three types of losses in MFTs: magnetic losses, windings losses and dielectric losses. The magnetic losses are the result of complex phenomena inside magnetic materials (hysteresis, eddy currents) and are therefore very complex to model physically. That is why empirical models based on measurement are used in transformer design. Because magnetic induction will not be sinusoidal due to converter voltages waveform, the improved generalized Steinmetz equation (IGSE) is used [8]. The windings losses are mainly due to Joule losses, but because of the high switching frequency, skin and proximity effects will induce parasitic eddy currents leading to additional losses. To take these effects into account, a model adapted to this geometry (Litz cables in core-type) has been developed, showing better performances than traditional Dowell model in this case [9]. Finally, the dielectric losses are calculated from the parasitic capacitances and the dissipation factor of the insulating material, considering each harmonic of the applied voltage.

For these losses calculations, the current and voltage shapes calculated in the first step are considered. A further improvement of the methodology consists in computing current and voltage shapes according to the leakage and magnetizing inductances calculated for each MFT.

Once the losses are known, a thermal calculation can be performed. A thermal network approach has been used. Conduction inside transformer parts (core, windings, resin) is taken into account via thermal resistances (electro-thermal analogy) calculated from intrinsic anisotropic thermal conductivities. Convection is considered on all transformer faces, and the convection coefficients are determined from empirical correlations. These correlations depend on the type of face, the fluid

velocity, the surface temperature and the fluid properties. Radiation is considered only for external transformer faces (radiating outwards) and is determined using Stefan-Boltzmann law. Because the thermal resistances and the hotspot locations depend on temperatures, an iterative process is used to determine maximal temperatures.

In the end, potential MFT designs are filtered to exclude the ones that do not respect performance criteria (inductances value, maximal volumes and weight) or maximal allowed temperature.

Finally, losses in MOSFETs are calculated. Conduction losses are calculated with the RMS currents obtained from analytical expressions related to the current shapes in Fig. 3 and the leakage and magnetizing inductances of every MFT (thus the process described above to solve the differential equations is performed a second time) and considering that $R_{ds,on}$ varies according to the temperature as in Eq. (1) [10],

$$R_{ds,on}(T_j) = R_{ds,on_{ref}}(T_{ref}) \left(\frac{T_j}{T_{ref}} \right)^{2.4} \quad (1)$$

where T_j is the junction temperature and $R_{ds,on_{ref}}$ is the MOSFET resistance given in the datasheet when the junction temperature equals T_{ref}. Turn-off losses are calculated by approximating the losses given by the datasheet by a second order polynomial. These losses are considered independent from the temperature. Turn-on losses are neglected because ZVS operation is assumed.

Finally, knowing the MOSFET losses, the base plate temperature and the thermal resistance of the power module, a new junction temperature is calculated. Then some iterations are performed to compute losses and junction temperature. The design with the best efficiency is finally selected.

4 Parameters and results

The methodology presented in the previous section is used with the following parameters to obtain the results shown in this section.

The power supply voltage is supposed to be 25 kV at 50 Hz and the rated power at the DC bus is 2 MW in traction mode. The DC traction bus and the DC intermediate bus voltages are 1.8 kV. Thus, 23 active PEBBs plus one for redundancy are needed.

The structure considered for MFTs is Core-Type constituted by two windings around two columns, with two C-shaped cores either in ferrite or nanocrystalline material, windings in laminated Litz cables (strands of 0.1 mm diameter), cast epoxy resin insulation and forced air cooling at 2 m/s. The ambient temperature equals 40 °C. The volume and weight for all the MFTs are limited to 450 dm^3 and 450 kg.

The power modules are from CREE/Wolfspeed, the base plate temperature is 100 °C. The dead time duration equals 1 µs. For DAB mode, the minimum time-shift at rated power equals 2 µs while the phase-shift is limited to 60 °.

For SAB mode, the ratio between the resonant frequency and the switching frequency equals 0.85 and 1.15 in CCM and DCM respectively and the voltage drop is limited to 10 % of the intermediate bus voltage. This voltage is highly dependent on the AC link resistance which is quite difficult to estimate in a preliminary study. For this work a AC link resistance of 100 mΩ is considered.

For each considered frequency, the efficiency at rated power of the best DC/DC converter is shown in Fig. 5. In a general manner, the curves show a maximum. If the switching frequency is too low, as the volume is limited, the core section is also limited and the induction is large, leading to high core losses. If the switching frequency is too high, switching losses, losses due to skin and proximity effects and core losses increase. The curves are quite ”flat”: if the best efficiency is obtained for a switching frequency close to 10 kHz, designing a MFT for a 20 kHz switching frequency does not lead to dramatic reduction of the efficiency. This is an important consideration, especially if noise standards can not be complied at the optimal switching frequency.

For ferrite cores, no solution satisfying the requirements were found for R-DAB nor with a frequency lower than 12 kHz. For nanocrystalline cores, thanks to their high saturation flux density, solutions were found at lower frequencies.

When results are obtained, nanocrystalline cores present best efficiencies than ferrites whatever the switching frequency and whatever the considered variant. For both ferrite and nanocrystalline, the

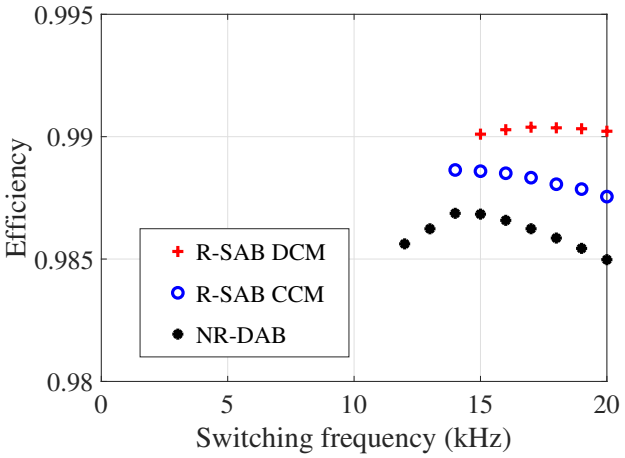

(a) Ferrite core

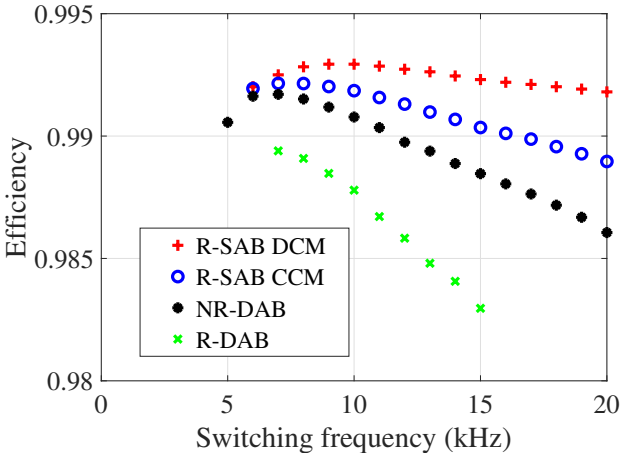

(b) Nanocrystalline core

Fig. 5: Efficiency at rated power of the best DC/DC converter found for each considered frequency

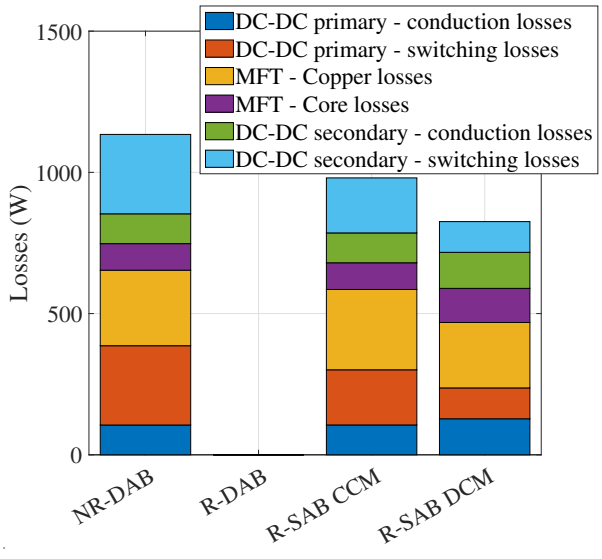

(a) Ferrite core

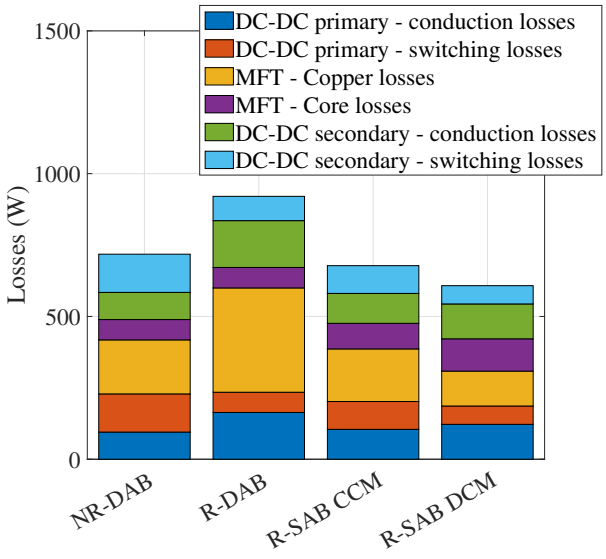

(b) Nanocrystalline core

Fig. 6: Losses in the DC/DC converters that allow the best efficiency at rated power

best efficiency at rated power is obtained in R-SAB DCM, R-SAB shows best efficiencies than DAB modes and R-DAB presents the poorest efficiency.

In any case, the efficiency is quite good and significantly better than with low frequency transformers and inverters usually used in such applications.

For all the solutions showing the best efficiency at rated power, the distribution of losses is shown in Fig. 6. The dielectric losses are negligible and, thus, not represented here.

It should be noted that the quite low conduction losses are related to the high rating of the power modules. Indeed, currently available 3.3 kV power modules from Wolfspeed present a $R_{ds,on}$ at 25 °C of only 5 mΩ [11] and a rated current of 450 A while the considered RMS current in this application is in the range of 50 A. Results should be quite different if considering power modules with a rated current more adapted to the considered application (power modules with less dies).

For a given variant, core losses and conduction losses are in the same range for ferrite cores and for nanocrystalline cores. But, as the optimal switching frequency for ferrite core solutions is larger than the one for nanocrystalline cores, the switching losses in MOSFETs and winding losses are higher for converters with ferrite cores.

The R-SAB DCM shows the best efficiency because it exhibits the lower switching losses (the model assumes no losses in turn-on (ZVS) and, at turn-off, the switched current is as low as the magnetizing current).

For nanocrystalline cores, losses in semiconductors are low even with the high considered base plate temperature. Indeed, in every DC-DC topology, the increase of the junction temperature of the MOSFETs is lower than 5 °C.

In the transformers, the winding and core temperatures highly vary with the design. The highest temperature, obtained in the windings of the nanocristalline MFT designed for a resonant DAB, reaches the temperature limit (fixed at 150 °C). However, in the other MFTs, the core and winding temperatures are comprised between 115 °C and 140 °C.

Forced air cooling for both power modules and MFTs can thus be considered. Compared to liquid cooling, which is generally used in railway applications, this would be a significant improvement for the maintenance.

For all the solutions with the best efficiency at rated power, the efficiency for various operating points is plotted in Fig. 7. It is shown that, even at low power, solutions with nanocrystalline cores offer better efficiencies than solutions with ferrite cores. One can also see that in any of the cases, the variant that shows the best efficiency at rated power, i.e. R-SAB DCM, exhibits the poorest efficiency at low power. For very low power, the best efficiency is obtained by the solution with nanocrystalline and R-DAB. At low power, the conduction losses are highly reduced, compared to the switching and core losses. This result is thus due to higher core losses in the MFT designed for R-SAB DCM applications than in the other MFTs. Then, as the converter will not operate always at rated power, the selection of the variant should consider weighed losses corresponding to a typical journey.

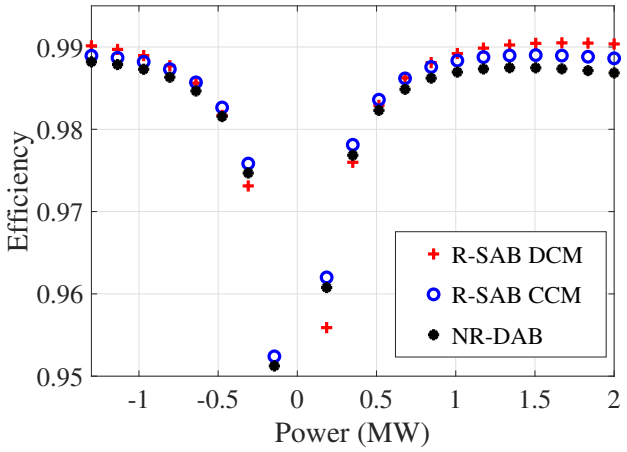

(a) Ferrite core

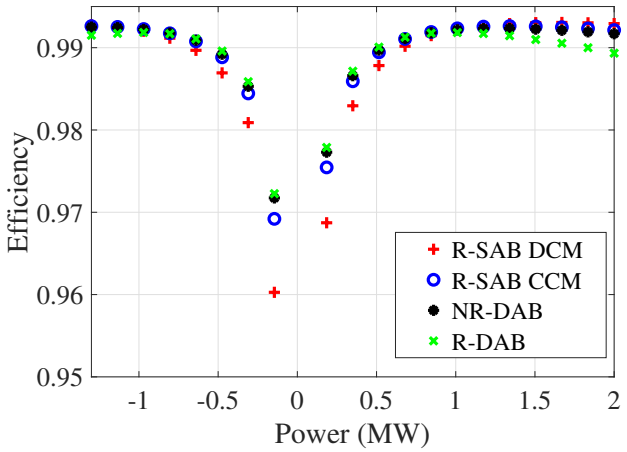

(b) Nanocrystalline core

Fig. 7: Efficiency according to the output power of the DC/DC converters that allow the best efficiency at rated power

5 Conclusion

This paper presents a method to size a DC/DC converter included in a PETT that leads to the best efficiency at rated power in a given volume. For 25 kHz / 50 Hz systems, among the considered variants, the R-SAB DCM shows the best performance at rated power. For each variant, the switching frequency that minimises the losses is quite low (a few kHz), even with SiC switches, and the best magnetic material is nanocrystalline. Nevertheless, other variants offer close efficiencies and even best efficiencies at low power. Losses in power module are low enough to consider forced air cooling instead of liquid cooling.

Finally to make a clear choice, efficiency can not be the only parameter; some other parameters should be discussed. For example, on the one hand, in NR-DAB there is no resonant capacitor, so both reliability and cost are improved. On the other hand, in R-SAB mode, there is no high constraint on the computing unit (no short time shift to control

with precision): the converter operates at fixed frequency and the AFEC controls V_{int} in order to control the transmitted power. So the cost of the computing unit can be reduced. Another parameter should be the acoustic noise, even if it is difficult to take it into account in preliminary studies. The results obtained in the study show that, according to the models, designing converters with a switching frequency in the range of 20 kHz would not lead to a dramatic reduction of the efficiency.

A perspective for this work consists in optimising converters not only for rated power but for a typical journey. A prototype would be also useful to validate models.

6 Acknowledgment

This work has been supported by a grant overseen by the French National Research Agency (ANR) as part of the “Investissements d’Avenir” Program (ANE-ITE-002-01).

References

[1] M. Mermet-Guyennet, “New power technologies for traction drives”, in *International Symposium on Power Electronics, Electrical Drives, Automation and Motion (SPEEDAM)*, 2010.

[2] D. Dujic, F. Kieferndorf, F. Canales, and U. Drofenik, “Power electronic traction transformer technology”, in *7th International Power Electronics and Motion Control Conference (IPEMC)*, 2012.

[3] S. Farnesi, M. Marchesoni, and L. Vaccaro, “Advances in locomotive Power Electronic systems directly fed through AC lines”, in *International Symposium on Power Electronics, Electrical Drives, Automation and Motion (SPEEDAM)*, 2016.

[4] B. Bednar, P. Drabek, and M. Pittermann, “The comparison of different variants of new traction drives with medium frequency transformer”, in *International Symposium on Power Electronics, Electrical Drives, Automation and Motion (SPEEDAM)*, 2016.

[5] J. Feng, W. Q. Chu, Z. Zhang, and Z. Q. Zhu, “Power Electronic Transformer Based Railway Traction Systems: Challenges and Opportunities”, *IEEE Journal of Emerging and Selected Topics in Power Electronics*, vol. 5, no. 3, 2017.

[6] T. Lagier and P. Ladoux, “A comparison of insulated DC-DC converters for HVDC off-shore wind farms”, in *International Conference on Clean Electrical Power (ICCEP)*, 2015.

[7] C. Stackler, F. Morel, P. Ladoux, A. Fouineau, F. Wallart, and N. Evans, “Optimal sizing of a power electronic traction transformer for railway applications”, in *International IEEE Conference on Industrial Electronics (IECON)*, 2018.

[8] K. Venkatachalam, C. R. Sullivan, T. Abdallah, and H. Tacca, “Accurate prediction of ferrite core loss with nonsinusoidal waveforms using only Steinmetz parameters”, in *IEEE Workshop on Computers in Power Electronics*, 2002.

[9] A. Fouineau, M. Raulet, B. Lefebvre, N. Burais, and F. Sixdenier, “Semi-Analytical Methods for Calculation of Leakage Inductance and Frequency-Dependent Resistance of Windings in Transformers”, *IEEE Transactions on Magnetics*, vol. 54, no. 10, 2018.

[10] K. Sheng, “Maximum Junction Temperatures of SiC Power Devices”, *IEEE Transactions on Electron Devices*, vol. 56, no. 2, 2009.

[11] J. Hayes, W. A. Curbow, B. Sparkman, D. Martin, K. Olejniczak, *et al.*, “Dynamic Characterization of Next Generation Medium Voltage (3.3 kV, 10 kV) Silicon Carbide Power Modules”, in *International Exhibition and Conference for Power Electronics, Intelligent Motion, Renewable Energy and Energy Management (PCIM)*, 2017.